Journal of Energy Storage 103 (2024) 114262

Contents lists available at ScienceDirect

Journal of Energy Storage

journal homepage: www.elsevier.com/locate/est

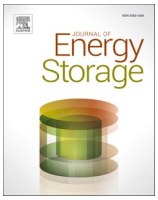

Research papers

An experimental and comparative study on passive and active PCM cooling of a battery with/out copper mesh and investigation of PCM mixtures

Umut Ege Samancıoğlu [a], Sinan Göçmen [a], Seyed Saeed Madani [b], Carlos Ziebert [b], Fernando Nuno [c], Jack Huang [d], Frank Gao [d], Erdal Çetkin [a,*]

[a] Department of Mechanical Engineering, Izmir Institute of Technology, Turkey
[b] Institute for Applied Materials – Applied Materials Physics (IAM-AWP), Karlsruhe Institute of Technology (KIT), 76344 Eggenstein-Leopoldshafen, Germany
[c] European Copper Institute, Avenue de Tervueren 168 b-10, 1150 Brussels, Belgium
[d] International Copper Association, Room 2582, 25F, 381 Huaihai Zhong Road, Huangpu District, Shanghai 200020, China

A B S T R A C T

The carbon emission contribution to global warming accelerated both research on and transition to electric vehicles (EVs). Drivers demand high power, fast acceleration and less charging times. All these demands require high C rate charging/discharging demands from batteries. The rate of heat generation is exponentially proportional to C rates which decreases battery lifetime and may lead to thermal runaway. However, a battery thermal management system decreases thermal runaway risk and decelerates battery degradation via controlling battery temperature. In this paper, we first document the thermal conductivity enhancement via copper foam into phase change material (PCM) domain to uncover their possible use in EV thermal management applications. Maximum 15.93 times increment is achieved with a specific copper foam. Then, physical properties and behaviors of distinct PCM mixtures are documented. Homogeneity of mixtures is associated with the chemistry of PCMs and the mixture melting point is proportional to the volume weighted average of melting temperatures. The results document that the PCM with relatively lower melting point is beneficial when end of discharge temperatures considered, except for high discharge rate of 2C. Temperature uniformity across the battery increases with relatively higher melting point PCM. Experiments also document that the amount of PCM volume lost via insertion of copper foam yields higher end of discharge temperatures. Overall, both PCM and copper foam enhances temperature homogeneity and their benefit becomes more sensible during drive cycles relative to continuous charge/discharge use cases.

1. Introduction

Harmful emissions such as CO_2 and NO_x caused by the internal combustion engine (ICE) vehicles can be reduced greatly with the electrification [1]. The efficiency of the vehicles calculated from the energy source (oil well or power plant) to distance being travelled is greater in electric vehicles (EV) relative to ICE vehicles [2]. Especially in the regions where the electricity is generated via renewable sources, that may yield the emissions for transportation to be reduced to zero. Because of these advantages, there is an increased interest over EV's [1–3]. According to International Energy Agency reports, many developed countries are progressively abandoning ICE vehicles and transiting to EVs by enforcing carbon emission regulations and offering financial and political incentives [4]. The need to store electricity in bulk quantities more efficiently took attention to the development of battery technologies. In EVs (both hybrid and battery only electric vehicles) currently used battery chemistries can be listed as lead-acid, nickel-cadmium (NiCd) and lithium-ion (Li-ion). However, Li-ion batteries are the most preferred choice in the automotive industry because of their higher energy density, no memory effect, lower self-discharge, longer life cycle and higher recyclability than competing chemistries [3,5–7].

Li-ion batteries can be divided into three categories according to their geometries: cylindrical, prismatic and pouch. Cylindrical batteries have high energy density, but the cylindrical shape creates redundant empty spaces that lowers the energy density of the complete battery pack. Pouch and prismatic cells possess a larger heat transfer surface area than cylindrical cells which makes them the most preferred li-ion battery type for high power EV's. However, the limited heat transfer capability of prismatic cells limits the battery thermal management capacity compared to pouch cells. In the near future pouch cells are expected to be the preferred choice due to these reasons [8].

Heat is generated within a Li-ion battery during charge and discharge processes. The generation of heat is non-uniform. The negative and positive tabs of the batteries heat up more than the other surfaces during charging and discharging, respectively. Furthermore, the temperature of a battery varies according to its thickness. The heat generation is related with the applied current on the cell and increases with increasing C-rate [9]. The generated heat causes temperature increment on the battery cell that result in increased capacity fade, aging and performance

* Corresponding author.
E-mail address: erdalcetkin@iyte.edu.tr (E. Çetkin).

https://doi.org/10.1016/j.est.2024.114262
Received 19 March 2024; Received in revised form 27 August 2024; Accepted 15 October 2024
Available online 24 October 2024

Nomenclature

A	ampere
Ah	ampere hour
Al	aluminum
BTMS	battery thermal management systems
cm	centimeter
C rate	current rate
EV	electric vehicle
g	gram
ICE	internal combustion engine
K	Kelvin
Li-ion	lithium ion
m	meter
NiCd	Nickel Cadmium
NMC	Nickel Manganese Cobalt
PCM	phase change material
PTB	National Metrology Institute of Germany
THB	transient hot bridge
W	watt

degradation, further elevation of the temperature may lead to serious safety problems such as thermal runaway [10]. In addition, uneven generation of heat creates hot spots on the cell that produce thermal stress which is detrimental for the battery health [11]. Heat generation rate can be managed by limiting the C-rates, but this can be a temporary and undesired solution as this would mean prolonged charging time and decreased driving power capability for EVs, which contradicts the customer demands [12]. The need for high C rates shows the cruciality of the battery thermal management systems (BTMS) in EV applications. Li-ion batteries have a wide operating range of −20 °C–60 °C, however negative effects can be observed such as increase in capacity fade over 40 °C and lithium plating below −10 °C. The optimal operating range for the Li-ion batteries is given as 15 °C–35 °C [13,14]. Further attention should be given to the temperature distribution on the battery surface, as more than 5 °C variation can cause thermal stress related negative effects like premature aging of the battery. Hence, a BTMS should satisfy four critical tasks, removing heat from the cells while ensuring uniform temperature distribution on cell surface and in the battery pack, heating to prepare the batteries in extreme cold conditions, exhausting the possible hazardous gasses that may be emitted from the batteries and insulation to prevent the batteries from sudden temperature changes [15,16].

Battery thermal management systems are divided into two categories: active and passive systems. Active systems incorporate coolants to employ forced convection. These coolants can be in gaseous or liquid state. On the other hand, passive systems extract the excess heat by using phase change materials (PCM), heat pipes or simply by natural convection. Active systems require an additional energy supply and more complicated than their passive counterparts; however, they ensure a better control over the system compared to passive BTMSs [17,18].

In recent years, PCMs have gained significant attention for their applications in thermal energy storage, electronic cooling and construction. PCMs are substances that undergo a phase transition, such as melting or solidification, within a specific temperature range. Their unique capacity to store and release thermal energy during phase transition makes them particularly well-suited for managing temperature in a desired range in various applications, contributing to energy efficiency and sustainability. Since they use phase change process to extract and store heat they achieve near isothermal conditions and prevent any sudden changes in temperature with high latent heat, battery health is enhanced. In order to benefit from these advantages, melting/solidifying temperature of the selected PCM should be same or in vicinity of the operating temperature of the batteries [19,20]. The literature contains various articles that studies BTMS's with mixed and passive methods that includes PCMs. Mousavi et al. [21] utilized mini – channel cold plates and PCM, their ideal design yield 30 °C reduction in maximum battery temperature. They concluded that the hybrid cooling improved the temperature uniformity. Wu et al. [22] constructed a BTMS with flexible composite phase change material (FCPCM). Their tests showed that the maximum temperature decreased to 28.8 °C from 43.4 °C. The advantage of their system was reported as the ease of assembling and technical simplicity. Li et al. [23] aimed to uncover an optimization strategy to minimize the PCM weight in a BTMS. They worked on cylindrical Li-ion cells and studied the effects of geometrical variations on the PCM. Iqbal et al. [24] compared natural convection, forced convection and PCM cooling. They worked with a single cell at three distinct C-rates. Their results showed that cooling with PCM achieved 7.2 %, 25.3 % and 31 % reduction in battery temperature compared to natural convection for 1C, 2C and 3C rates, respectively. They conclude that PCM cooling is capable of controlling the temperature successfully without any external power requirement, and it is the most effective method based on their study. Javani et al. [25] experimented with the PCM shell thickness for prismatic cells. They conducted a numerical study where the shell thicknesses change from 3 mm to 12 mm gradually. Simulation results showed that as PCM thickness increases surface temperature and temperature excursion of the batteries decrease. They also document that with 3 mm PCM thickness battery surface temperature uniformity enhances by 10 %. Isfahani et al. [17] studied passive and mixed cooling strategies. They proposed a combination of microchannels, and metal foam induced PCM then this setup was compared with BTMSs that consist of only metal foam induced PCM or microchannel. Their results revealed that only PCM yields a more uniform temperature distribution than the only microchannel but the maximum temperature of the battery is greater in the only PCM than the only microchannel. On the other hand, the hybrid system yields the lowest maximum temperature for a cell with enhanced temperature uniformity than the system with only microchannels. Mo et al. proposed a PCM module for cooling and preheating batteries in all climate conditions. They incorporated composite PCM (CPCM) with sleeve like units to enhance the airflow and heat transfer surface. Results showed the thermal resistance decreased by 52.0 % and 60.1 % for cooling and preheating modes and the heat flux increased 7 times compared to base case. Also, satisfactory preheating and cooling performances were reported with minimal temperature variance between individual cells. Lv et al. investigated the durability of PCMs for long term applications. CPCM is preferred in the experiments and experimented for 200 charge-discharge cycle. At 200th cycle the maximum temperature was 4.2 °C lower than no PCM case with only 0.6 °C individual cell temperature difference. When the impedance, micro/crystal structure characterization and internal resistance of the cells investigated positive effects of PCM on cathode stability and cell consistency shown in the article with a proposed 65.3 % enhanced cycle life. Jilte et al. utilized nanoparticle enhanced phase change materials (nePCM) with two distinct two-layer PCM design. nePCMs are PCM materials doped with conductive nano particles like metals or metal oxides to enhance thermal conductivity of PCM. Design alternatives differed from if the nePCM geometries are individual cylinders wrapping cells or produced as single block. They uncovered that radial layering is more beneficial compared to axial layering, individual cylinder design is more effective compared to the alternative and lower temperature nePCM should be placed closer to the cells when layered structure is used. They managed to preserve the batteries even in high ambient temperature of 40 °C with only 6 °C temperature increment.

This study uncovers the effect of copper foam insertion into a PCM domain both from the material characterization and experimental battery thermal management perspectives. This paper documents the complete process for PCMs as a component in BTMS applications from thermal characterization, PCM mixture creation and characterization,

passive cooling effectiveness via experiments in various load conditions and active/passive cooling effectiveness in combination with liquid cooling. The battery thermal management literature focuses on active and/or passive (such as PCM) thermal management strategies without documenting the benefits and burdens associated with them. This paper aims to compare both approaches for the same application in order to document both benefits and burdens associated with them to uncover the applicability in distinct applications.

The novelty of this paper is associated with its aim of uncovering the PCM/copper foam performance in a battery thermal management by uncovering fundamental behaviors and then experimentally uncovering their performance in a realistic condition in application which is missing in the literature. Thus, thermal characterization experiments for copper foam, sole PCMs and copper foam induced PCM are documented. Then, the behaviors of various PCM mixtures are studied to document the possibility of uncovering unique PCM mixtures, which is not common in the literature. To create a realistic cooling behavior, various PCMs and copper foam effects were uncovered employing cyclic heat generation to mimic driving characteristics as well documenting continuous charge/discharge behaviors.

2. Characterization of thermal properties of PCM combined with copper foam

2.1. Methodology

For thermal conductivity measurements the DRH tester (flat-plate heat protection, Xiangtan Xiangyi Instrument Limited Company) was used at European Copper Institute (ECI) and the THB-100 system from Linseis company at Karlsruhe Institute of Technology (KIT). The DRH test is based on the principle of stable heat conduction, one-way heat flows vertically through the plate sample in steady state. The thermal conductivity of the sample can then be calculated by measuring the one-dimensional constant heat flow in the specified heat transfer area and the temperature difference between the hot and cold surfaces of the sample. Fourier's law is used to calculate thermal conductivity which is as follows:

$$\lambda = \frac{W \bullet d}{A \bullet (T_1 - T_2)} \quad (1)$$

The THB-100 is shown in Fig. 1 and works with the Transient Hot Bridge method, which is a heating wire process optimized by the National Metrology Institute of Germany (PTB), with which the thermal conductivity and specific heat capacity can be measured. The thermal conductivity measurement range extends from insulation materials to ceramics and metals. The THB method employs a bridge sensor that serves as both the heat source and temperature sensor, simplifying the experimental setup and ensuring accuracy when dealing with PCMs in various states (solid, liquid, and gelled). The bridge sensor both heats the sample and monitors temperature changes. Both the sample, which should be flat to ensure a good thermal contact, and the bridge sensor are encased by the sample holder, which is shown on the right side of Fig. 1. The sample holder is then surrounded with insulating material to minimize heat loss to the surroundings. The next step is to initiate the process by cooling the sample to a temperature below its phase change point, usually in its solid state, to establish well-defined initial conditions and to apply a short, constant electrical pulse to the bridge sensor to heat it. The temperature changes over time are recorded as heat is conducted through the PCM. The bridge sensor will cool down as heat is conducted into the PCM, and the rate of cooling depends on the thermal conductivity of the PCM. Finally, the recorded data are analyzed to determine the thermal conductivity of the PCM. Typically, this involves fitting the temperature response curve to a mathematical model that relates the rate of cooling to thermal conductivity.

2.2. Characterization of copper foam

The thermal conductivity of the pure copper foams with different porosities were measured using the DRH tester. The results are shown in Table 1. For the experiments in this work copper foam samples with approximately A4 size, a density of 0.45 g/cm^3, a porosity factor ε of 94.94 % and a thermal conductivity λ of 4.21 W·m^{-1}·K^{-1} have been provided by ECI. Fig. 2 shows one of these samples.

2.3. Characterization of PCMs

Thermal conductivity is a fundamental property significantly affecting PCM performance, since it reflects a material's ability to conduct heat. Accurate measurement of PCM thermal conductivity is vital for comprehending their heat transfer characteristics and optimizing their utility. It is worth noting that the accuracy of measurements with the transient hot bridge system may depend on various factors, including the experimental setup and the specific PCM being tested. Careful calibration and consideration of potential sources of error are essential for obtaining precise results. Additionally, combining this system with other analytical techniques can provide a comprehensive characterization of PCM properties.

2.4. Characterization of compounds with PCM and copper mesh

Some preliminary measurements on compounds based on paraffin as a simple PCM with the copper foam and different amounts of graphite have been performed, which are shown in Table 2. The amount of

Table 1
Thermal conductivity of copper foams with different porosities as determined by DRH tester.

Density (g/cm^3)	Porosity factor ε	Copper foam thermal conductivity λ (W·m^{-1}·K^{-1})
0.60	93.26 %	5.76
0.45	94.94 %	4.21
0.35	96.17 %	2.91
0.25	97.79 %	1.72

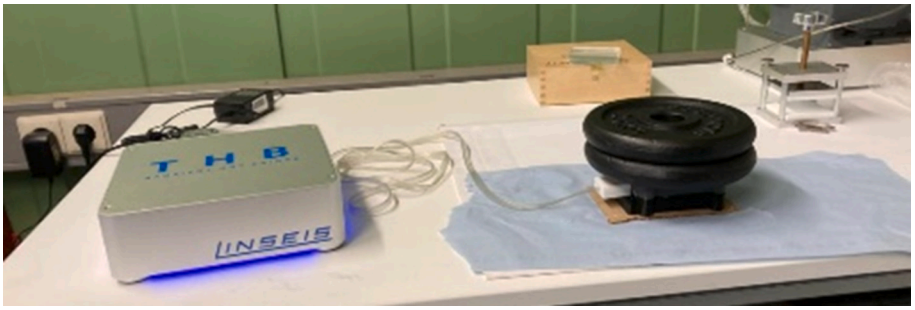

Fig. 1. Thermal hot bridge THB-100 system from Linseis for thermal characterization.

Fig. 2. Photo of copper foam sample.

Table 2
Latent heat and melting point of paraffin + copper foam + epoxy resin + different amounts of graphite.

Serial number	Composite material components	Latent heat/J/g	Melting point/°C
1	Pure paraffin + copper foam + epoxy resin	202.5	47.84
2	1 % graphite + pure paraffin + copper foam + epoxy resin	180.4	47.95
3	3 % graphite + pure paraffin + copper foam + epoxy resin	131.9	47.91
4	4 % graphite + pure paraffin + copper foam + epoxy resin	129.2	47.84
5	5 % graphite + pure paraffin + copper foam + epoxy resin	115.9	47.52

graphite is calculated as mass percent in the experiments. It turns out that the melting point is almost unaffected whereas the latent heat decreases by 40 % when 5 % of graphite is added. Which is caused by reduction of PCM amount in the compound because the specific heat of the graphite is lower than the PCM even the total mass is the same.

The thermal conductivity of empty epoxy resin was determined to be 0.208 $W{\cdot}m^{-1}{\cdot}K^{-1}$ (Table 3). The effect of copper foam on the effective thermal conductivity increment with the epoxy resin is given in Table 4. It shows that copper foam is able to increase the thermal conductivity to 2.242 $W{\cdot}m^{-1}{\cdot}K^{-1}$, which is a factor of 10.78. In addition, the thermal conductivity of pure paraffin was determined with the DRH tester as 0.21 $W{\cdot}m^{-1}{\cdot}K^{-1}$. The addition of the copper foam increased the thermal conductivity of the composite material by a maximum of 15.93 times, reaching to 4.3 $W{\cdot}m^{-1}{\cdot}K^{-1}$.

Tables 5, 6, 7 and 8 show the measurement results for PCM materials RT42, RT38, RT35HC and SP31 from Rubitherm GmbH with embedded copper foam, respectively. RT42 is a pure PCM with a melting area between 38 °C and 43 °C and a heat storage capacity of 165 kJ/kg, RT38 is a pure PCM with a melting area between 34 °C and 39 °C and a heat storage capacity of 165 kJ/kg, and RT35HC is a pure high capacity PCM with a melting area between 34 °C and 36 °C and a heat storage capacity of 240 kJ/kg. The RT35HC possesses a higher latent heat capacity of 25–30 % compared to the classic RT materials RT38 and RT42 and melts

Table 3
Thermal conductivity of pure Epoxy Resin as determined by THB-100 tester.

Measurement	Thermal conductivity $W{\cdot}m^{-1}{\cdot}K^{-1}$
1	0.20746
2	0.20722
3	0.20856
Average value	0.20775

Table 4
Thermal conductivity of Epoxy Resin with embedded copper foam as determined by THB-100 tester.

Measurement	Thermal conductivity $W{\cdot}m^{-1}{\cdot}K^{-1}$
1	2.0459
2	1.7312
3	4.3735
4	2.0554
5	2.1181
6	1.2919
7	2.9749
8	1.3475
Average value	2.2423

in a narrower temperature range, which is advantageous in cases in which a limited volume exists. SP31 is a low-flammability PCM consisting of a combination of inorganic components and is corrosive to metals. The comparison shows that RT38 with embedded copper foam has the highest thermal conductivity of 0.33 $W{\cdot}m^{-1}{\cdot}K^{-1}$, whereas SP31 exhibits the lowest with only 0.07 $W{\cdot}m^{-1}{\cdot}K^{-1}$.

3. PCM mixtures

3.1. Methodology

The possibility of benefitting from the properties of distinct PCMs is questioned by conducting experimental studies on PCM mixtures. Four distinct PCM alternatives, namely, RT25HC, RT35HC, SP31 and PX38 by Rubitherm GmbH are considered. PCMs with melting temperature range of 25–38 °C investigated in this article since this range is representative to the optimal range required for maximizing the lifetime of li-ion batteries [13,14]. A total of three mixing experiments were conducted with RT25HC – RT35HC, RT25HC – SP31 and RT25HC – PX38 couples. RT25HC, RT35HC and SP31 are in solid form where PX38 is in powder form. The PCMs were mixed in 200 ml beakers with equal amounts (100 ml each in solid phase). The beakers were heated with an electric heater from the bottom until the mixture temperature reaches 50 °C to homogenously mix the materials. Then the mixture was allowed to cool by natural convection in 20 °C environment while their temperature variation was measured at 5 distinct points across the height of the beaker. K – type thermocouples were connected to HIOKI-LR8431–20 datalogger to measure and record the temperatures at 0 ml, 50 ml, 100 ml, 150 ml and 200 ml levels of the beaker for a 3600 s period. The three mixing experiments are demonstrated in Fig. 3 with temperature measurement points.

3.2. Results and discussion of the PCM mixing experiments

The first mixing experiment was conducted with RT25HC – RT35HC PCM couple. The Fig. 4 presents the temperature recordings of the RT25HC – RT35HC at specified measurement points.

The data show that the mixture started to solidify at approximately 30 °C. It is specified as “Solidification starts” indicator in Fig. 4. This is notable, since the arithmetic average of the melting points of the RT25HC – RT35HC PCMs is exactly 30 °C. This suggests that when the RTHC series PCMs are homogenously mixed at desired proportions, a new PCM with adjusted melting temperature can be produced. In addition, further melting and solidification of this mixture revealed that the new PCM is able retain its properties and does not show any separation when melted. It is also important to mention that the thermocouples placed at 0 ml and 200 ml points recorded lower temperatures compared to the rest of the thermocouples. This is caused by the combined effects of exposure to ambient air and start of solidification on outer faces of the PCM.

Next, mixture of the RT25HC – SP31 PCM couple was investigated.

Table 5
Thermal conductivity of RT42 PCM with embedded copper foam.

Measurement	Tempera-ture °C	Tempera-ture Δ °C	Measure-ment time	Heating current	Thermal conductivity $W{\cdot}m^{-1}{\cdot}K^{-1}$	Thermal diffusivity mm^2/s	Cp $J{\cdot}K^{-1}{\cdot}kg^{-1}$
1	25.62	1.53	30	50	0.1930	0.0634	3461.22
2	25.68	1.52	30	50	0.1947	0.0662	3340.81
3	25.71	1.52	30	50	0.1953	0.0711	3120.48
Average value	25.67	1.52	30	50	0.1943	0.0669	3307.48

Table 6
Thermal conductivity of RT38 PCM with embedded copper foam.

Measurement	Tempera-ture °C	Tempera-ture Δ °C	Measure-ment time	Thermal conductivity $W{\cdot}m^{-1}{\cdot}K^{-1}$	Thermal diffusivity mm^2/s
1	18.01	1.94	20	0.3233	0.3256
2	18.04	1.89	20	0.3293	0.2486
3	18.03	1.86	20	0.3293	0.2466
4	18.05	1.84	20	0.3288	0.2378
5	18.02	1.81	20	0.3292	0.2336
6	18.01	1.79	20	0.3292	0.2293
7	18.04	1.73	20	0.3299	0.2268
8	17.98	1.76	20	0.3290	0.2241
9	18.02	1.71	20	0.3283	0.2241
10	18.00	1.71	20	0.3283	0.2286
11	18.05	1.72	20	0.3296	0.2290
12	18.00	1.68	20	0.3304	0.2276
13	18.02	1.65	20	0.3311	0.2268
14	18.02	1.64	20	0.3308	0.2290
15	17.97	1.66	20	0.3319	0.2294
16	18.00	1.66	20	0.3314	0.2275
17	18.03	1.65	20	0.3313	0.2294
18	18.07	1.62	20	0.3319	0.2267
19	18.04	1.63	20	0.3316	0.2288
20	18.06	1.62	20	0.3319	0.2230
21	18.09	1.57	20	0.3324	0.2217
22	18.02	1.60	20	0.3314	0.2222
23	18.04	1.59	20	0.3312	0.2261
24	18.03	1.62	20	0.3320	0.2216
25	18.00	1.58	20	0.3318	0.2236
26	18.04	1.55	20	0.3322	0.2250
27	18.05	1.54	20	0.3313	0.2243
28	18.08	1.58	20	0.3314	0.2226
29	18.08	1.53	20	0.3313	0.2226
30	18.02	1.56	20	0.3318	0.2215
Average value	18.03	1.68	20	0.3304	0.2313

The mentioned PCMs were placed in a beaker and heated with the same procedure as in RT25HC – RT35HC PCM couple. However, the RT25HC – SP31 PCM couple did not produce a homogenous mixture. RT25HC floated over SP31 in the beaker. The heterogenous mixture of RT25HC – SP31 couple is shown in Fig. 5 with homogenous mixture of RT25HC – RT35HC PCMs for comparison. The separation interface is also indicated in Fig. 5.

The mixture was then heated above the maximum allowable limit of SP31 PCM to uncover the behavior of the materials when their limits are exceeded. This experiment revealed that SP31 was incapable of phase change after its temperature exceeded the limit value (60 °C) and did not solidify even below 20 °C. Further waiting showed, after approximately 24 h at room temperature SP31 can solidify again. An additional melting experiment uncovered SP31 regained its phase change abilities as normal. However, this is an essential result as exceeding a limit temperature may eliminate thermal management capability of some PCMs in EV battery thermal management applications. In conclusion this experiment unveiled the problems related with heterogenous PCM mixtures such as incomplete mixing, phase separation, and density-driven segregation.

Lastly, the RT25HC – PX38 PCM couple was studied. PX38 is a heat storage powder using hydrophilic silica powder as a secondary support structure. The mixture of RT25HC – PX38 couple did not form a homogenous mixture. The PX38 absorbed some of the liquid RT25HC and sank to the bottom of the beaker. Further experimentation with the mixing ratios showed that a more homogenous mixture can be achieved, however using these PCMs separately would be advised depending on the application.

To sum up, the mixing experiments demonstrated that for homogenous mixtures of RTHC series PCMs can be used for preparation of a special PCM with desired melting temperature. PCMs with different chemistries are not suitable for preparing such mixtures. Exceeding the allowed limits of a PCM may cause it to temporarily lose its phase change properties. In the experiments 24 h was required for PCM to regain its solidification ability; however, this behavior of the SP31 showed the importance of conformity of the limit properties of a material and the application.

4. Passive cooling tests using PCM filled plastic containers with/out copper foam

4.1. Methodology

Two distinct PCM's were used in the passive cooling tests with PCM filled plastic containers. The selected PCM's were RT25HC and RT35HC that supplied from Rubitherm GmbH. PCM blocks were produced with the selected PCM's with or without using a copper foam insert. In total 4 distinct PCM blocks were produced and tested comparatively. Produced

Table 7
Thermal conductivity of RT35HC PCM with embedded copper foam.

Measurement	Tempera-ture °C	Tempera-ture Δ °C	Measure-ment time	Thermal conductivity $W{\cdot}m^{-1}{\cdot}K^{-1}$	Thermal diffusivity mm^2/s
1	18.18	2.27	20	0.2356	1.7534
2	18.18	2.28	20	0.2376	1.7771
3	18.21	2.27	20	0.2399	1.7483
4	18.26	2.24	20	0.2419	1.7265
5	18.23	2.20	20	0.2439	1.7161
6	18.22	2.24	20	0.2455	1.7138
7	18.21	2.20	20	0.2472	1.7010
8	18.17	2.20	20	0.2483	1.6919
9	18.19	2.19	20	0.2492	1.6759
10	18.22	2.16	20	0.2504	1.6767
11	18.19	2.19	20	0.2511	1.6665
12	18.20	2.17	20	0.2519	1.6673
13	18.16	2.17	20	0.2525	1.6657
14	18.16	2.15	20	0.2530	1.6553
15	18.18	2.23	20	0.2538	1.6561
16	18.19	2.17	20	0.2547	1.6518
17	18.19	2.16	20	0.2548	1.6438
18	18.17	2.16	20	0.2554	1.6399
19	18.19	2.21	20	0.2560	1.6485
20	18.14	2.18	20	0.2565	1.6374
21	18.20	2.16	20	0.2570	1.6382
22	18.18	2.18	20	0.2574	1.6358
23	18.18	2.18	20	0.2576	1.6494
24	18.12	2.19	20	0.2581	1.6437
25	18.15	2.15	20	0.2587	1.6294
26	18.18	2.15	20	0.2589	1.6241
27	18.13	2.16	20	0.2584	1.6281
28	18.14	2.15	20	0.2580	1.6402
29	18.21	2.13	20	0.2582	1.6484
30	18.17	2.16	20	0.2579	1.6497
Average value	18.18	2.19	20	0.2520	1.6700

Table 8
Thermal conductivity of SP31 PCM with embedded copper foam.

Measurement	Tempera-ture °C	Tempera-ture Δ °C	Measure-ment time	Thermal conductivity $W{\cdot}m^{-1}{\cdot}K^{-1}$	Thermal diffusivity mm^2/s
1	18.01	4.52	20	0.0699	3.2151
2	18.01	4.48	20	0.0698	3.2163
3	18.02	4.50	20	0.0700	3.2490
4	17.99	4.51	20	0.0701	3.2071
5	18.00	4.49	20	0.0701	3.1385
6	18.00	4.50	20	0.0703	3.1775
7	18.03	4.49	20	0.0703	3.1680
8	18.00	4.50	20	0.0704	3.1565
9	18.01	4.48	20	0.0705	3.1145
10	17.96	4.49	20	0.0705	3.1218
11	18.00	4.48	20	0.0705	3.1888
12	18.00	4.49	20	0.0705	3.1403
13	18.01	4.50	20	0.0705	3.1517
14	18.04	4.52	20	0.0705	3.1637
15	18.03	4.53	20	0.0705	3.1692
16	18.00	4.52	20	0.0704	3.1994
17	18.00	4.50	20	0.0704	3.2419
18	17.97	4.49	20	0.0704	3.2157
19	17.96	4.46	20	0.0704	3.1933
20	18.00	4.47	20	0.0704	3.2294
21	17.95	4.49	20	0.0704	3.2528
22	17.94	4.49	20	0.0703	3.2789
23	17.92	4.50	20	0.0703	3.2976
24	17.97	4.48	20	0.0704	3.2287
25	17.91	4.52	20	0.0704	3.2552
26	17.97	4.50	20	0.0704	3.2416
27	17.94	4.48	20	0.0704	3.3078
28	17.97	4.50	20	0.0704	3.2784
29	17.93	4.49	20	0.0703	3.3148
30	17.95	4.46	20	0.0703	3.2799
Average value	17.98	4.49	20	0.0703	3.2133

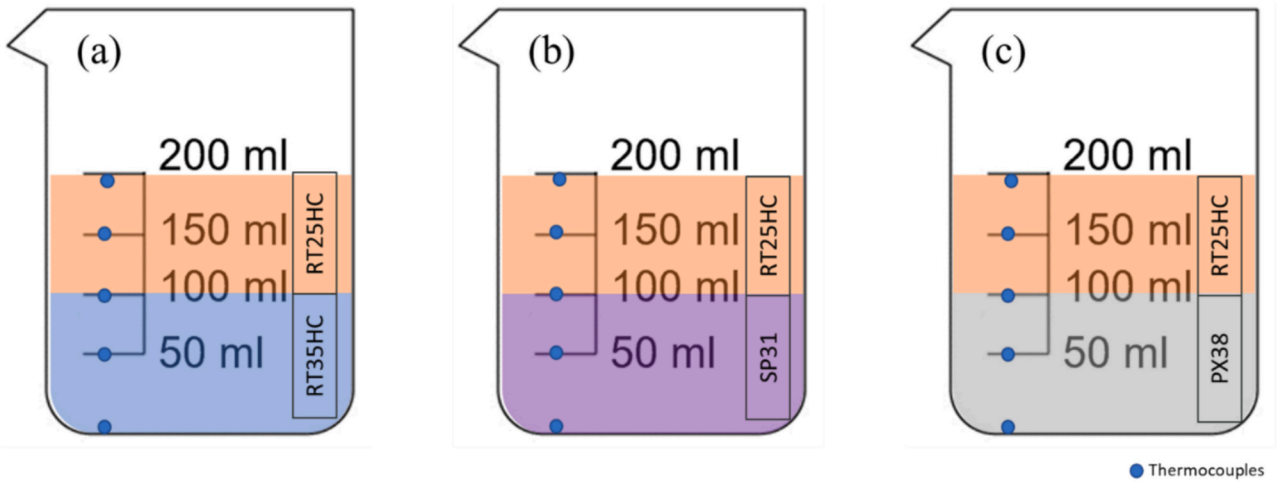

Fig. 3. Mixing experiment demonstration with thermocouple placements.

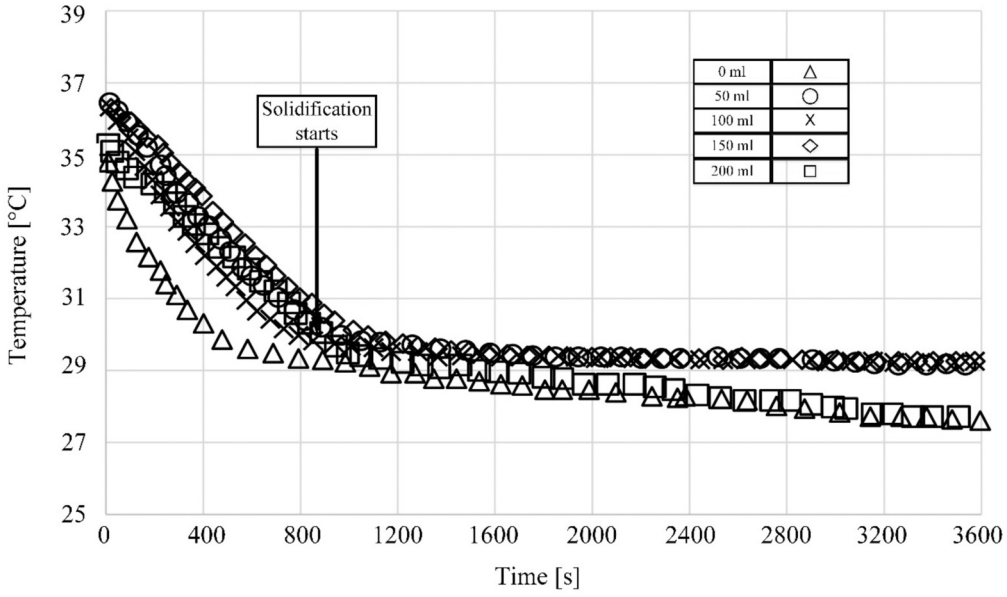

Fig. 4. RT25HC - RT35HC mixture temperature results.

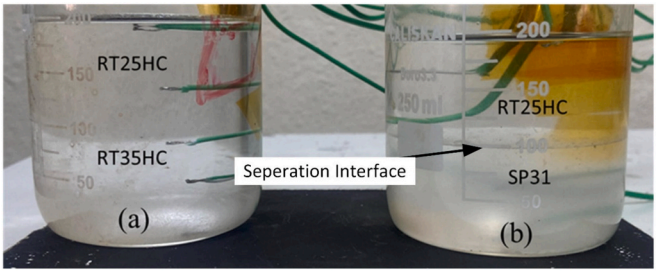

Fig. 5. RT25HC - SP31 mixture comparison with RT25HC - RT35HC mixture.

blocks tested in discharge tests conducted with NMC pouch cells. A mold was constructed to produce PCM blocks. Dimensions of the PCM blocks are 104 mm width, 295 mm length, and 5 mm thickness.

After the mold was created with desired dimensions, the copper foam was inserted as in Fig. 6.

Mold, copper foam (if exists) and PCM canister are placed in an oven at 50 °C. Molten PCM is poured in the mold then waited for the PCM to solidify, Fig. 7a. Produced PCM block is removed from the mold as in Fig. 7b and wrapped with heat resistant vacuum bag and fixed with vacuum tape in Fig. 7c. The copper foam is always on the surface of the battery and kept away from the tabs of the battery to prevent any short circuit, also the vacuum bag in which the copper foam/PCM is located ensured the electrical insulation of the copper foam.

After the PCM block is produced, the block is placed on top of the battery, then the battery-PCM block couple is insulated from both sides as in Fig. 8. K-type thermocouples are placed on specified places and connected to HIOKI-LR8431-20 data logger to measure and record the temperatures. Three thermocouples are placed in between insulation and PCM block (positive tab side (6), middle (7) and negative tab side (8) of the battery), two thermocouples placed in between PCM block and NMC pouch cell (positive table (1) and negative table (2) sides), one thermocouple placed in between the back of the battery and insulation (3) and the tab temperatures are measured with 4th and 5th channels for positive and negative terminals, respectively. Places of the thermocouples are shown in Fig. 8.

The battery is connected to the BK Precision 8614 programmable electronic load for the discharge tests. The electronic load is used to

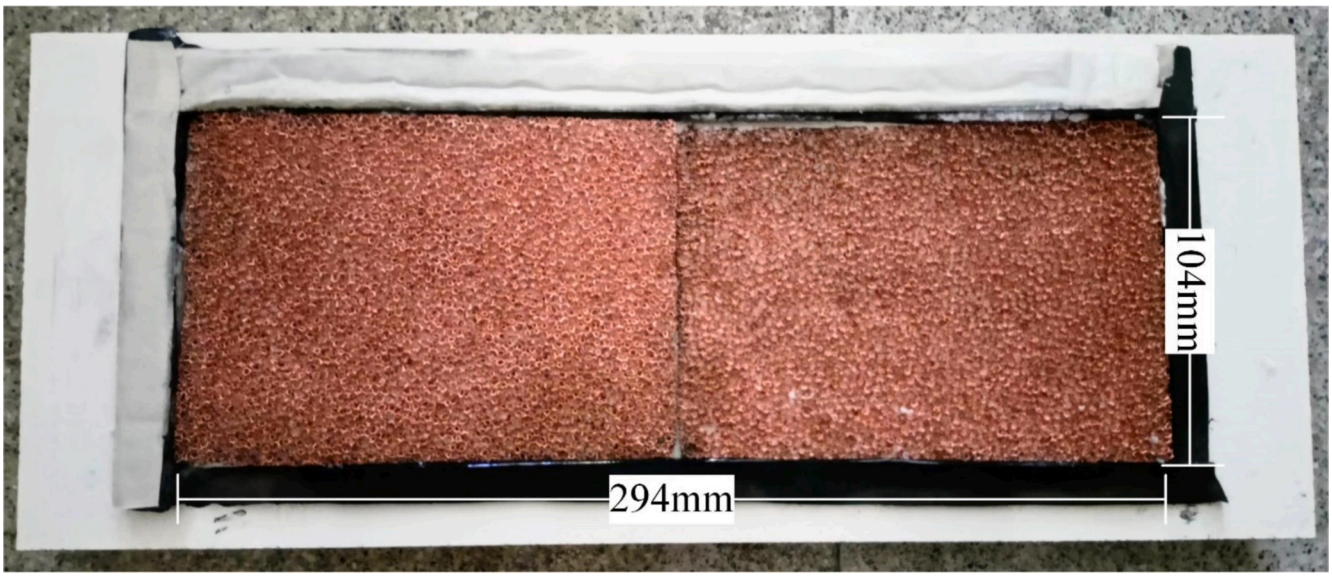

Fig. 6. The PCM mold and copper foam with dimensions.

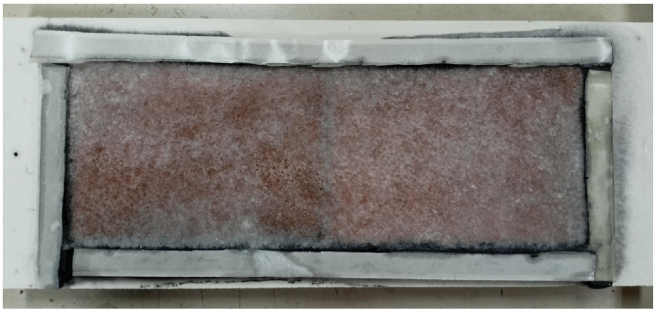

(a)

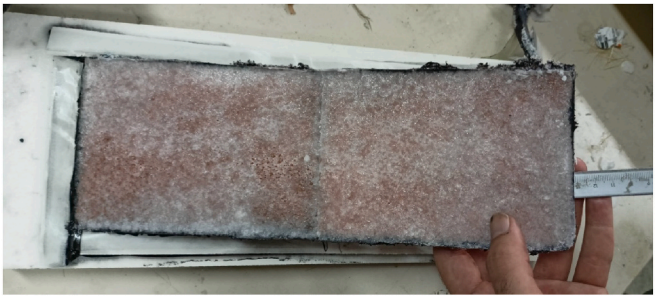

(b)

(c)

Fig. 7. PCM block production a) solidified PCM block in the mold, b) removal of PCM block from the mold and c) PCM block wrapped in vacuum bag to produce PCM block.

discharge the NMC pouch cell at 1C-rate (73 A), 2C-rate (146 A) and with a simulated cyclic discharge procedure (given in Table 9). The temperatures were then recorded using the HIOKI-LR8431-20 data-logger. The complete test setup is presented in Fig. 9.

4.2. Results and discussion

In the following part, PCMs with distinct melting temperatures are used to uncover the effect of PCM melting temperature on the battery's heating behavior. In the experiments, RT25HC and RT35HC are used for this purpose. PCM blocks with copper foam are produced and placed in containers made from vacuum bag and tape.

Three cases, without PCM, RT25HC with copper foam and RT35HC with copper foam, and three points, middle of the PCM block (7), positive side of the battery - PCM block interface (1) and middle of the battery and insulation interface (3) are investigated to lay out the benefits of using PCM and effect of PCM melting point. The graphs are based on the gradient relative to the ambient temperature to eliminate the effect of ambient temperature fluctuation.

Fig. 10 displays the temperature values of the selected points for 1C rate discharge. The selected points are, the middle of the PCM block - insulation interface (7), positive tab side battery (1) and PCM block interface and middle of the battery - insulation interface (3). Fig. 10 demonstrates that as a general trend using a PCM block greatly helps to manage the excess heat generated by a battery under constant discharge. Case without any PCM block reaches higher temperatures through the discharge process and have approximately 10 °C higher end of discharge temperature. Examination of the PCM block temperatures reveals that with 1C rate discharge, heat storage capacities of the PCM blocks are not completely used. As, there are no sudden increment in the Fig. 10 for the PCM block temperature values. Comparing the RT25HC and RT35HC PCM blocks shows that, for 1C rate RT25HC is able to keep the temperatures of the battery lower compared to RT35HC. This is caused by the higher melting point of the RT35HC. The RT35HC requires battery to generate more heat in order to be effective, phase change does not occur. This is visible by the characteristics of the temperature measurements from (3) and (1) for RT35HC. The data suggests that at approximately 36 °C RT35HC started to melt and extract heat from the PCM battery interface. Maximum temperature variation between the two faces of the battery for systems with RT25HC and RT35HC are 4.2 °C and 2.3 °C, respectively, where this variation for no PCM case was measured as 5.4 °C. These results show us that the RT35HC is considerably more

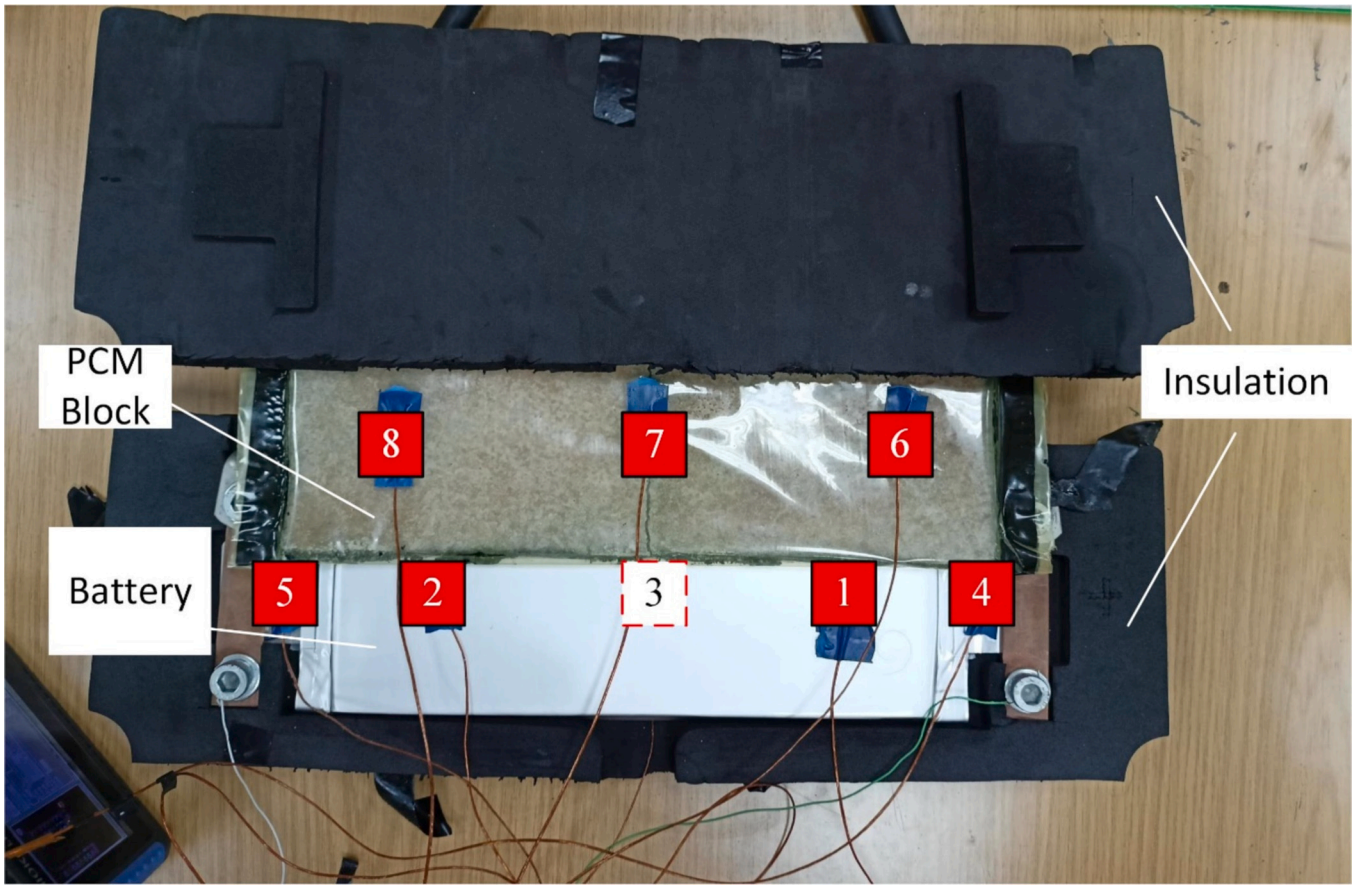

Fig. 8. Battery, PCM block and insulations with thermocouple locations.

Table 9
Cyclic discharge C-rates and durations.

Discharge rate[C]	Duration[s]
1	60
0.5	60
Rest	30
1.5	120
2	120
0.5	180
Rest	30

beneficial to use when the uneven thermal stress on the battery is considered. Lastly, even though at 1C-rate discharge RT25HC kept the battery temperatures at the lowest, relatively low melting point of RT25HC might cause problems at elevated ambient temperatures. Since most of its heat storage capacity might be already used by the high ambient temperature while in rest.

Fig. 11 displays the temperature values of the selected points for 2C rate discharge. For the no PCM case the experiment had to be stopped before completion since the battery temperatures passed the maximum allowed operation temperature limit of 60 °C. This proves the need of a cooling mechanism for 2C-rate discharge of this NMC pouch cell. Also, temperature difference between the cases with and without any PCM block is nearly doubled compared to 1C rate discharge case and approximately 20 °C at the end of discharge. The graph also shows the heat storage capacity of the RT25HC PCM block is completely used around 1600th second, this is suggested with the sudden increase in the PCM block temperature (7) for the RT25HC. With the depletion of the heat storage capacity of the RT25HC PCM block at 2C-rate discharge, RT35HC was able to keep the positive tab side battery temperature (1)

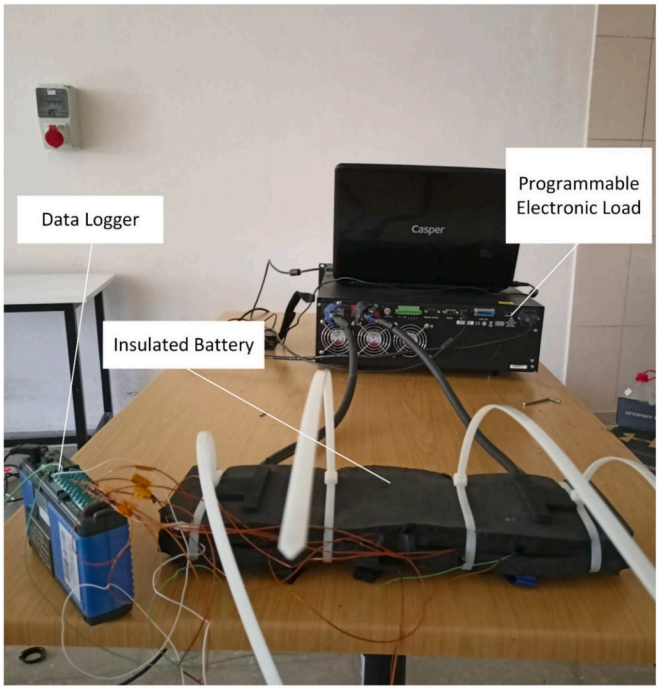

Fig. 9. PCM filled plastic containers experiments test setup.

lower compared to RT25HC after around 1600th second. For the insulated side of the battery, the two PCM block alternative showed similar temperature values. Maximum temperature variation between the two

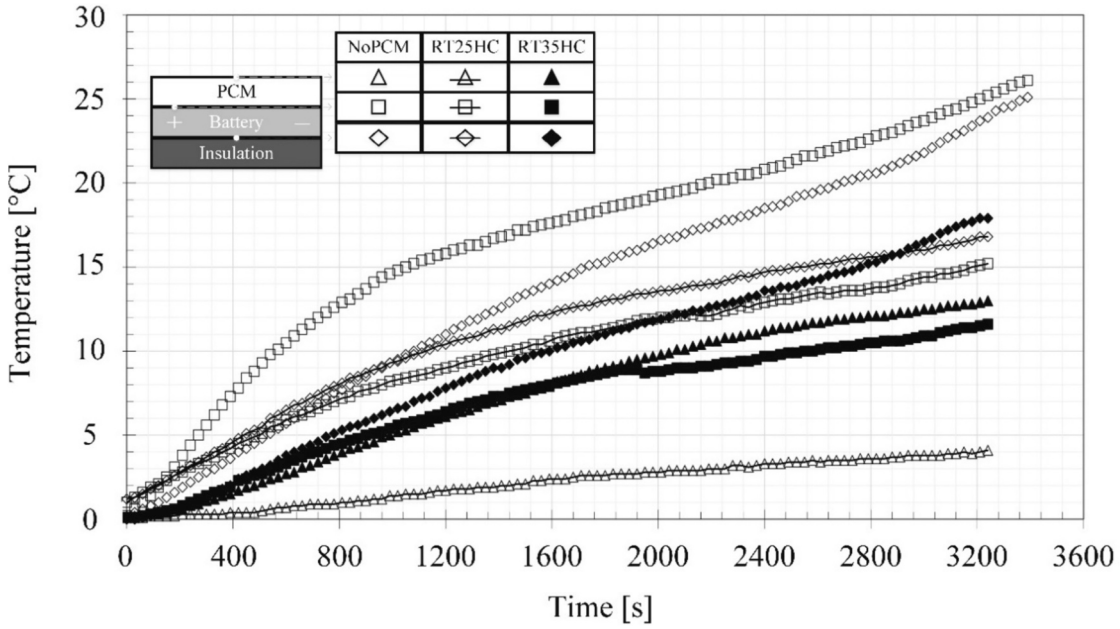

Fig. 10. Temperature values of the PCM block, PCM battery interface and battery for 1C-rate discharge with copper foam insert.

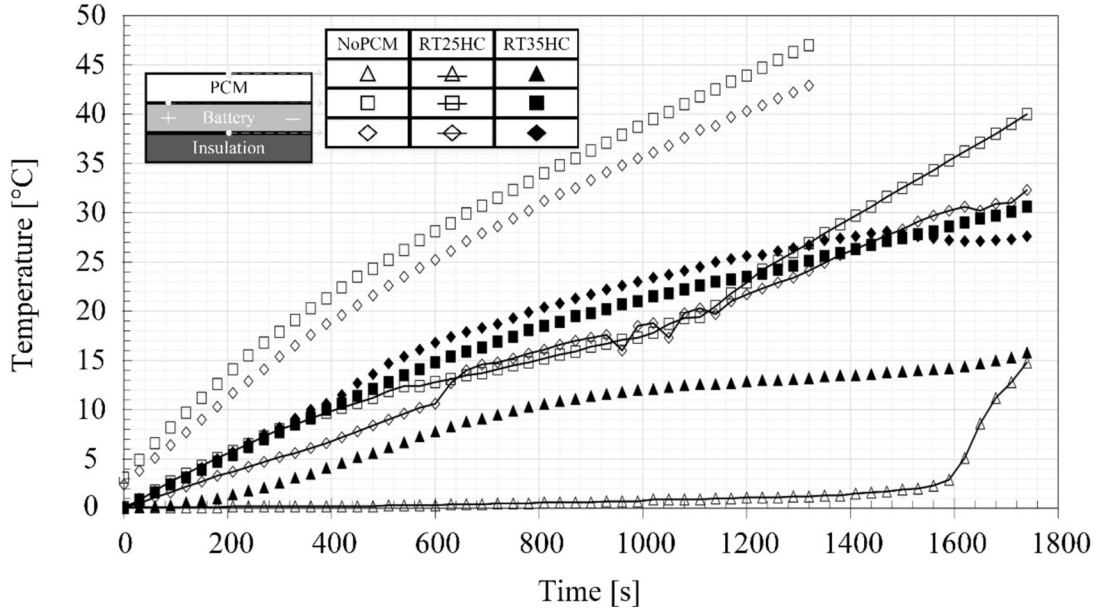

Fig. 11. Temperature values of the PCM block, PCM battery interface and battery for 2C-rate discharge with copper foam insert.

faces of the battery for systems with RT25HC and RT35HC are also very close for 2C rate discharge and noted as 7.3 °C and 6.6 °C, respectively. The temperature difference across the battery for no PCM case was measured as 9.8 °C. For the 2C rate discharge case the RT35HC is the most preferable alternative with lower end of discharge temperature, and same as 1C rate discharge case, for thermal stress consideration.

Fig. 12 presents the temperature values of the selected points for cyclic discharge. The temperature difference between the cases with and without a PCM block is calculated approximately 10 °C as the 1C rate discharge case. The PCM block temperatures (7) suggest that the cyclic discharge does not produce enough heat to deplete the heat storage capacities of the PCM blocks as in the 1C rate discharge case. This is evident since there are no jumps in temperatures values. When RT25HC and RT35HC PCM blocks are compared for cyclic discharge, RT25HC is able to keep the temperatures of the battery considerably lower compared to RT35HC. The cause of this behavior is the same as in the 1C rate discharge experiment and that RT35HC has a higher melting point which requires battery to reach to higher temperatures to be effective. With the cyclic discharge the PCM blocks are able to experience a little cooling effect in between the high discharge rates. This cooling effect benefits RT25HC more compared to RT35HC since it starts to melt and solidify earlier than the RT35HC due to its lower melting/solidification temperature. When the maximum temperature variation between the two faces of the battery for systems with RT25HC and RT35HC are calculated, it is seen that again RT35HC has a considerable positive effect on temperature uniformity across the battery. The maximum temperature difference values were calculated as 4.2 °C and 2.6 °C, respectively. This variation for no PCM case was calculated as 5.2 °C. In the end, for cyclic discharge RT25HC worked very effectively and kept the battery temperatures considerably low, however using RT35HC

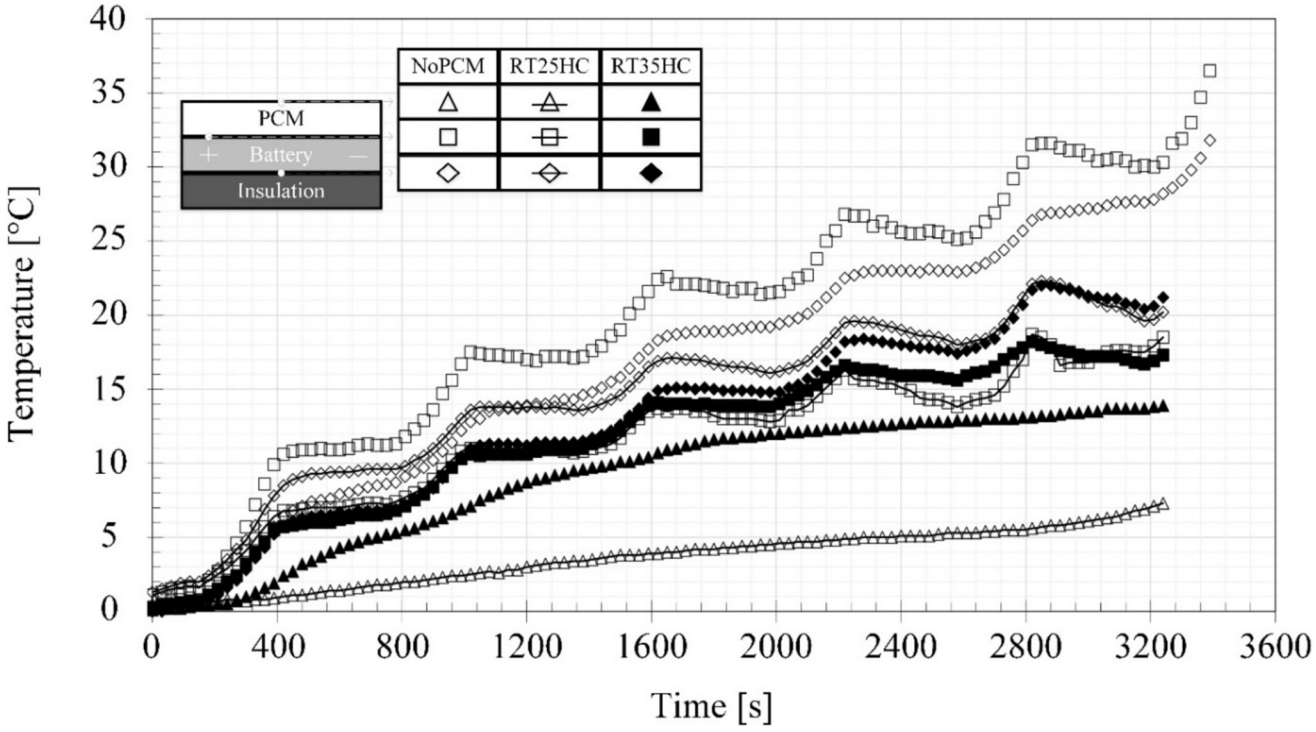

Fig. 12. Temperature values of the PCM block, PCM battery interface and battery for cyclic discharge with copper foam insert.

might be healthier for the battery when thermal stress effects are considered. Also, the probability of RT25HC to quickly lose its advantages at elevated ambient temperatures should be noted.

Next, the effect of copper foam insert inside the PCM block was investigated. In these experiments RT35HC was used with or without copper foam insertion. Battery heating behavior is observed with these alternatives under 1C, 2C rate and cyclic discharge.

Fig. 13 displays the temperature values of the selected points for 1C-rate discharge with PCM blocks that either has a copper foam or not. For cases that contain a copper foam "with CF" expression is used. The temperature graph in Fig. 13 shows that PCM block temperatures (7) are almost equal, and their difference is in the vicinity of 0.4 °C, where block without copper foam is relatively hotter. This can be related with copper foam to reject heat to lower heat generation zone of the battery more effectively and keeping the middle point relatively cooler. However, the temperature difference between the alternatives is very small. When the positive side battery – PCM container interface (1) and battery-insulation interface (3) temperatures for the PCM block alternatives are examined, the increase in temperature values related with copper foam used block is observed. Temperatures measured from both (1) and

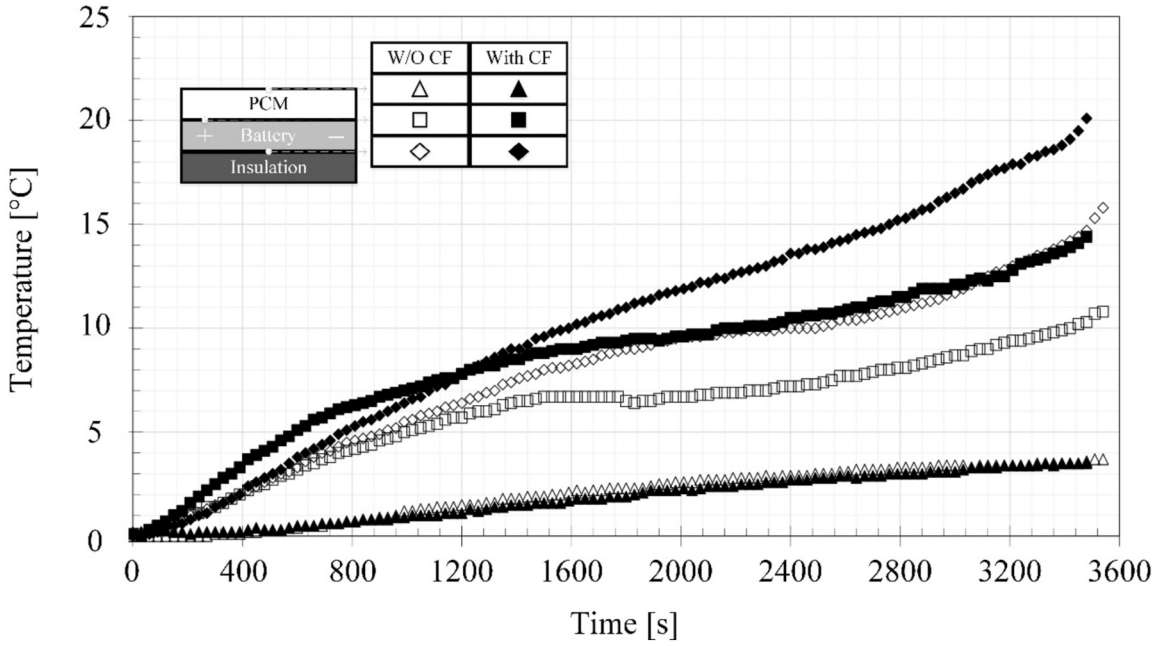

Fig. 13. Temperature values of the PCM, PCM battery interface and battery for 1C-rate discharge with and without copper foam insert.

(3) are lower for PCM block that does not contain any copper foam. There are distinct temperature differences between the end of discharge temperatures of the two PCM block alternatives as 2.9 °C and 4.3 °C at (1) and (3), respectively. This distinction between the alternatives originated from the constant volume mold. Because of the constant volume, including the copper foam inside decreases the total volume of PCM material in the PCM block with copper foam. This causes the same volume PCM block to have less heat storage capacity. The copper foam is expected to increase the thermal uniformity of the PCM block and achieve more efficient melting and solidifying, however at least in this case this is not possible to uncover. The decrease in heat storage capacity leads temperatures related to PCM block with copper foam insert to rise more steeply compared to PCM block without any copper foam insert.

Fig. 14 presents the temperature values of the selected points for 2C-rate discharge with PCM containers that either has a copper foam or not. PCM block temperatures are again almost equal with a 1 °C difference, where block without copper foam is relatively hotter. PCM block - battery interface temperatures (1) show that on the 800th second, the temperatures from the two alternatives start to differ. Same as in the 1C-rate case, PCM block without copper foam insertion enables lower temperatures for (1). Contrary to the PCM block - battery interface results and 1C-rate case there is no distinct difference between the PCM block alternatives for battery - insulation interface (3). This may be caused by the very high heat generation rate of the NMC pouch cell under 2C-rate discharge coupled with the incapability of conduction to transfer the heat across the battery from (3) to (1) where PCM blocks effectively to cools down. So, the similar temperature values of the (3) suggest that the process is limited by the conduction capacity across the battery rather than the PCM block's heat storage capacity.

In Fig. 15 the temperature results of cyclic discharge for RT35HC with and without a copper foam insertion has been given. When the temperature values of the battery in Fig. 15 studied, it is possible to notice that contrary to earlier experiments (1C-rate and 2C-rate) the PCM block with copper foam was performed better than its alternative. The temperature data from PCM block - battery interface (1) shows that the surface of the battery kept distinctly cooler with using copper foam until 2200th second. After this point the latent heat capacity of lower volume PCM in copper foam used block was filled, and temperature started to rise more quickly compared to the alternative. This distinction between the behavior of heating can be originated from the more uniform temperature distribution achieved by the copper foam inside the PCM block, that possibly allowed a more uniform melting and solidification process (as expected). This improvement in temperature uniformity is enabling the surface temperatures of the battery to go down even further by transferring the heat extracted from high heat generating sections on the battery across the PCM block to the low heat generation areas during low C rates or rest periods. The indistinct differences between the temperature measurements from battery - insulation interface (3) shows the positive effect of copper foam is limited to the applied surface and does not reduce the temperatures of the cell homogenously along its depth.

Further, length of the cooldown duration of the insulated battery is studied. Temperature increase of the battery was limited by storing the excess heat as latent heat in passive cooling with PCM blocks. Investigation of the effect of this stored latent heat on the cooldown time of the battery is important. The cooling down period of the cases with no PCM block and PCM blocks with/out copper mesh was investigated after 100 % discharge. For this purpose, temperatures were measured for 10 h after discharge was completed. Temperature behavior of the three alternatives namely, without any PCM block, RT35HC with copper foam insert and RT35HC without any copper foam insertion is examined.

The Fig. 16 shows the temperature measurement of the battery at the battery positive side - PCM block interface (1) over a 10-h long rest period. The temperature of the environment was at 28–29 °C in the experiments. The figure shows that the battery reaches the ambient temperature in 9 h regardless of using a PCM block or not. This is expected since the total energy generated by the battery during the discharge period is constant. These results prove the insulation of the battery is working well since there is no inexplicable loss of energy even with relatively high temperatures reached in case without any PCM block. Also, temperature data shows that after approximately 5.5 h the battery without any PCM block reaches the same temperature level as the cases with PCM blocks. Then the area in between the no PCM line and one of the lines corresponding to PCM block used cases is representative to the energy absorbed by the PCM block. When the temperatures related to cases that contain a PCM block are evaluated, it is possible to see that their behavior is nearly identical where only a 1 °C of difference exists at maximum. This difference originated from the higher PCM volume of the PCM block without any copper foam. Temperature behaviors of the cases with PCM blocks start with a sudden drop of temperature from +13 °C to +8 °C. Then a very long cooling period exists. On the other hand, the case without any PCM block starts from

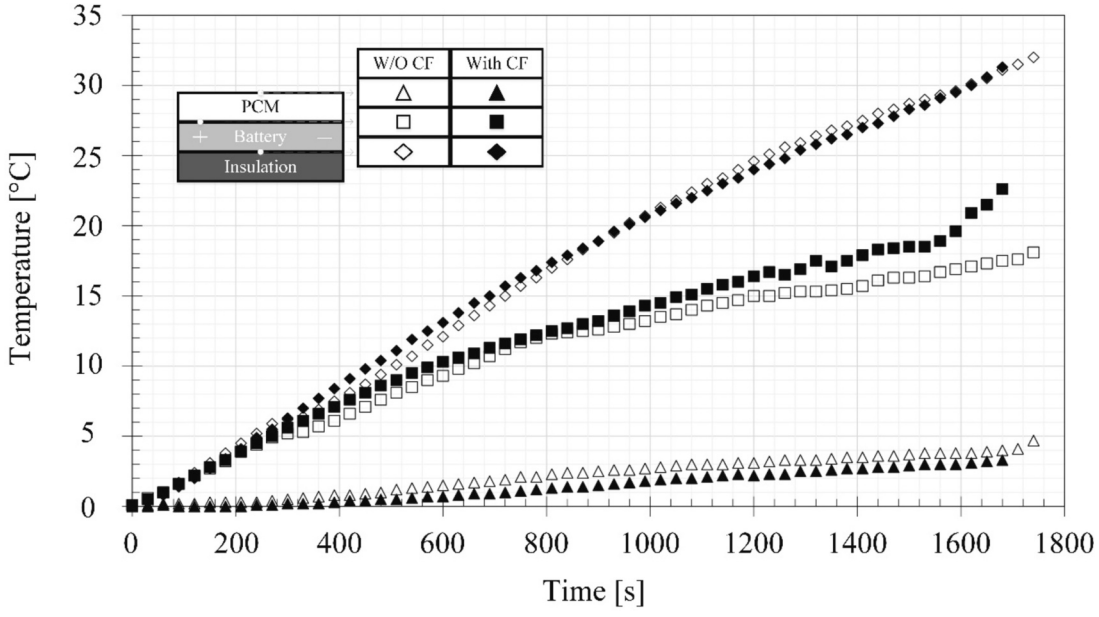

Fig. 14. Temperature values of the PCM, PCM battery interface and battery for 2C-rate discharge with and without copper foam insert.

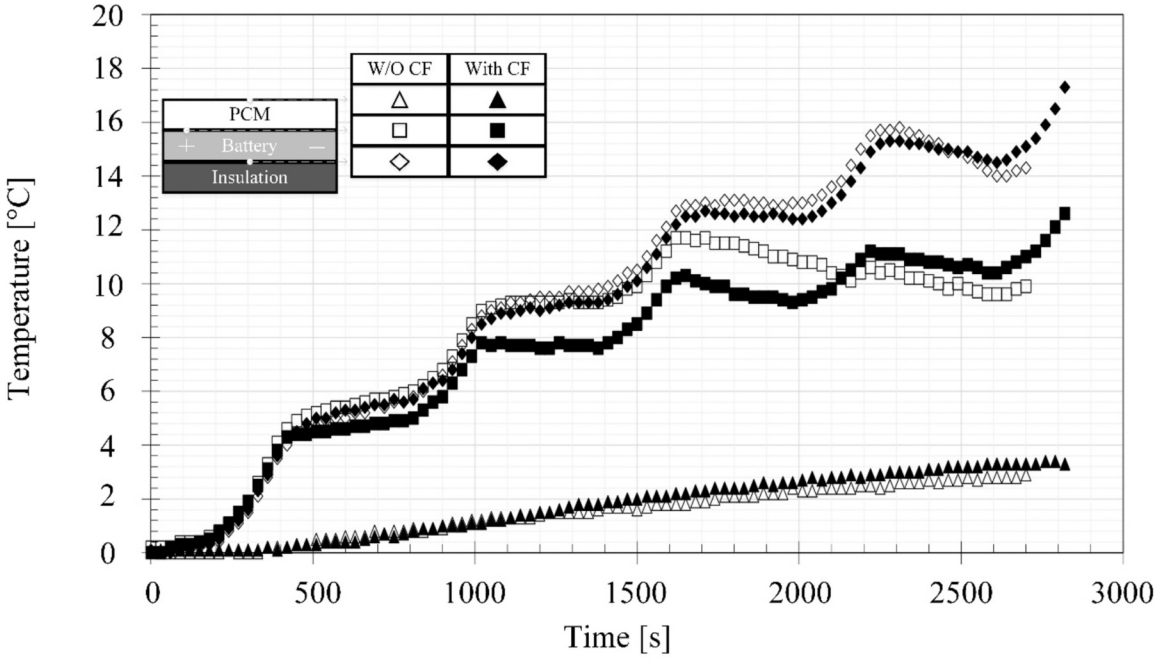

Fig. 15. Temperature values of the PCM, PCM battery interface and battery for cyclic discharge with and without copper foam insert (where results for PCM block with copper foam is increased by 2 °C to compare the performances).

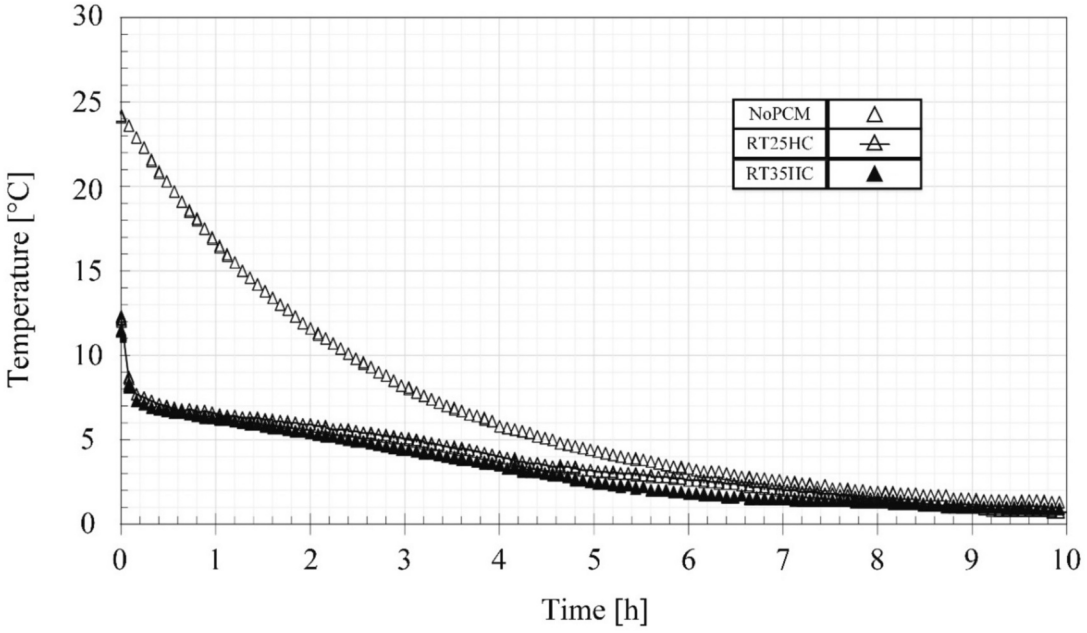

Fig. 16. Temperature variation of battery blocks during cooling down with the PCM block alternatives.

relatively high temperature at around +25 °C and shows a cooling graph with a steep slope where around 5 °C temperature drop per 1 h period experienced. When the thermal stress caused by the rapid change in temperature is considered, it is clear that using a PCM block is very beneficial for the battery health of the battery for both discharge and rest periods.

5. Passive cooling with PCM filled aluminum containers with/out liquid cooling

5.1. Methodology

Other sections show that even though copper foam increases the thermal conductivity of the PCM pack, when PCM packs are relatively thin, PCM pack without a copper foam can be more beneficial if the end of discharge temperature is considered. This leads the idea of using a thermally conductive casing material, such as aluminum, instead of using metal foam as the thermal resistance along the thickness of PCM pack would not change in sensible manner to affect melting

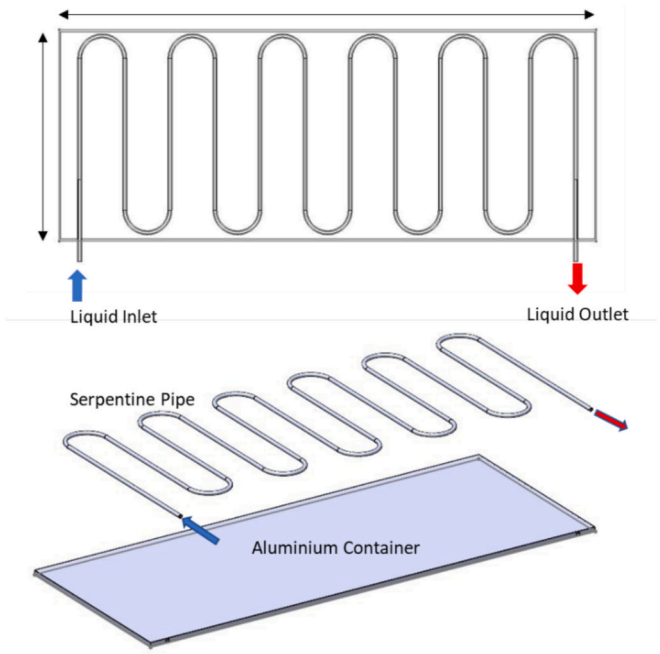

Fig. 17. Schematic of aluminum container with liquid cooling.

characteristics. While the effect of casing material is investigated, the passive and mixed cooling strategies are also studied, for this purpose two types of aluminum containers were produced. One of the containers involves a serpentine liquid channel for cooling and inside of the other container is just a cavity. Outer dimensions of the containers were 104 mm width, 265 mm length, and 7 mm thickness. For the serpentine, 6 mm diameter aluminum pipe is used. Schematic of the aluminum container with liquid cooling is presented in Fig. 17.

The produced containers were then filled with RT25HC and SP31 PCMs. The serpentine inside the container was connected to a water circulator to regulate the temperature. A 73 Ah NMC pouch cell was used as the heat source for testing. The battery was connected to the BK Precision 8614 programmable electronic load to be discharged at 1C – rate (73 A). The aluminum container was placed on the battery. Then, the battery and the container were insulated from both sides as in Fig. 18. For temperature measurements, K – type thermocouples were used at battery – insulation interface, battery – aluminum container interface and inside and outside of the aluminum container. The thermocouples were connected to HIOKI-LR8431–20 datalogger to measure and record the temperatures at specified points. The ambient temperature during these experiments was measured as 20 °C.

5.2. Results and discussion

In Fig. 19 temperature measurements for the two aluminum container alternatives with and without liquid circulation are presented. RT25HC was filled in the containers. The circulated liquid was liquid water at 20 °C and the ambient temperature was also measured as 20 °C.

Temperature data in Fig. 19 shows that the PCM temperatures of the two alternatives are recorded as 26.7 °C and 23 °C for PureRT25HC and RT25HC + LiquidCooling, respectively. The temperatures of the battery – aluminum container interface are 34.6 °C and 31 °C in the same respective order. The results clearly indicate the container with liquid cooling system is able to compensate the temperature increase from the heat generation more effectively. The temperature difference between the two alternatives is approximately constant on battery surface and inside the PCM block, this suggests that the difference originated purely because of the water circulation. The temperatures of the battery – insulation interface were recorded as 38.7 °C and 34.9 °C for PureRT25HC and RT25HC + LiquidCooling, respectively. There is an approximate 4 °C difference between the cooled and insulated faces of the battery. The 4 °C temperature difference across the battery may cause a thermal stress on the cell which is detrimental to its longevity.

In Fig. 20 temperature measurements for the two aluminum container alternatives with and without liquid circulation are presented. SP31 was filled in the containers. The circulated liquid was liquid water at 20 °C and the ambient temperature was measured as 18 °C for PureSP31 experiments and 20 °C for the experiments with liquid cooling.

In Fig. 20 the recorded temperatures of the PCM inside the containers are 28.6 °C and 23 °C for PureSP31 and SP31 + LiquidCooling, respectively. This suggests that SP31 was not melted since the temperatures did not reach the 31 °C level. The battery – aluminum container

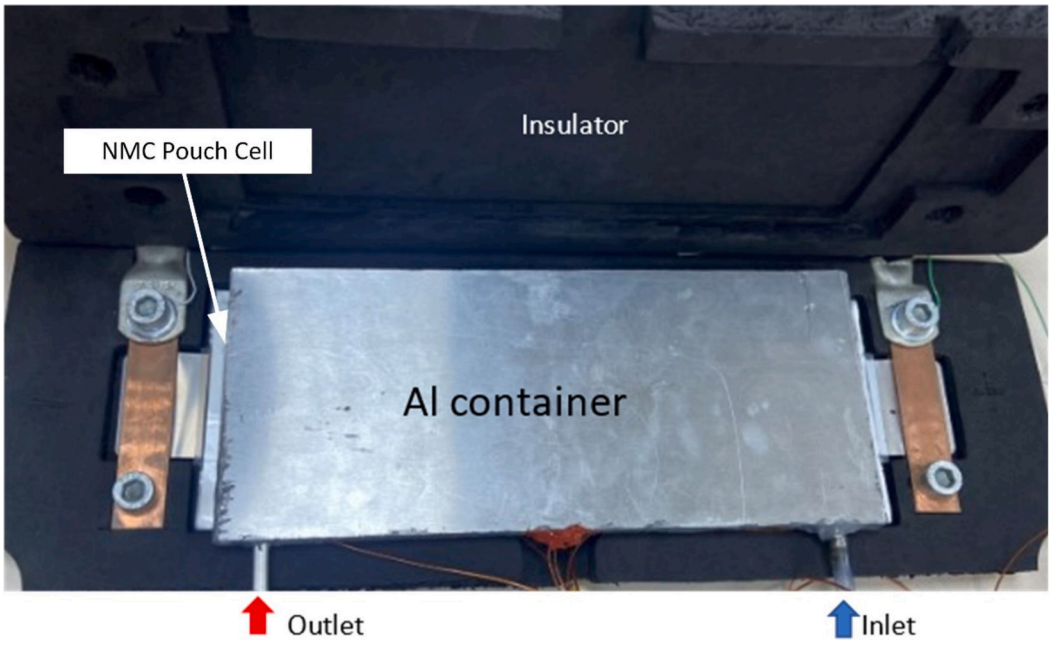

Fig. 18. Aluminum container experiments test setup.

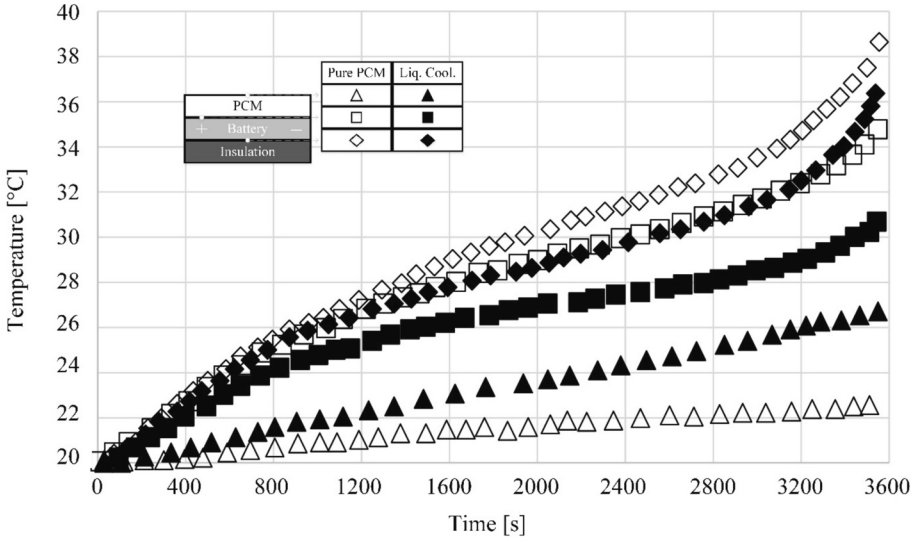

Fig. 19. Temperature variation for design with RT25HC filled Al container with/out liquid cooling.

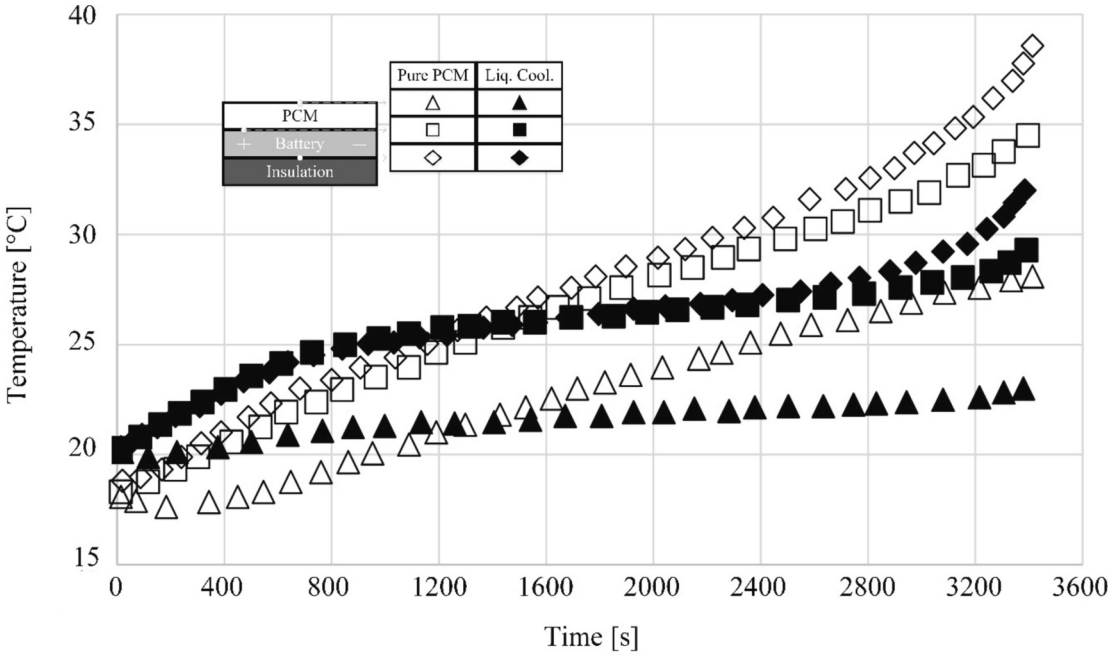

Fig. 20. Temperature variation for design with SP31 filled Al container with/out liquid cooling.

interface temperatures are given as 35 °C and 29 °C in the same respective order. Again, for PureSP31 and SP31 + LiquidCooling the temperatures on the battery – insulation interface are recorded as 39 °C and 32 °C, respectively.

The results show that the temperatures of the battery on both battery surfaces are nearly identical for the two PCM alternatives for pure PCM application, where only approximately 0.3 °C difference is present. When the PCM temperatures for the pure PCM design are investigated, the higher PCM temperature for SP31 alternative is visible. This suggests that RT25HC starts to melt earlier where the melting is not as significant with SP31. When the equal temperatures of the battery surfaces for both applications are considered, SP31 can be more advantageous with the reserved latent heat capacity. However, the ambient temperature difference between the two experiments should be noted which can cause this distinction. When the temperature data regarding the Liquid-Cooling + PCM is investigated, the indistinction between the two PCM alternatives can be seen. This indicates that the water circulation effect is more dominant than the PCM's heat storage capacity and the result is independent from the used PCM alternative.

To sum up, these experiments showed that liquid cooling is beneficial for battery thermal management, also liquid cooling is the dominant mechanism when used alongside PCMs. However, the increased complexity of the system with liquid cooling should be considered for the only 3.5 °C advantage it offers compared to pure PCM systems. Lastly, in both aluminum container design and for both PCM alternative an approximate 4 °C difference across the cell was measured, which can lead to premature aging of the battery. When thermal management system for a battery pack is considered, this thermal stress should be noted and prevented.

6. Conclusions

In this paper, possible use of PCM for electric vehicle battery pack thermal management is studied in four distinct parts; measurement of thermal conductivity of PCMs with embedded copper foam, PCMs as a mixture, melting temperature and copper foam effect, and finally passive and mixed cooling strategies comparison with aluminum containers are investigated. Outputs of the experiments are presented in the following paragraphs in the respective order.

Characterization experiments showed;

- Copper foam effectively increased the thermal conductivity of pure paraffin by 15.93 times, from 0.21 $W{\cdot}m^{-1}{\cdot}K^{-1}$ to 4.3 $W{\cdot}m^{-1}{\cdot}K^{-1}$.
- From PCMs of interest, the highest thermal conductivity with embedded copper foam was measured as 0.33 $W{\cdot}m^{-1}{\cdot}K^{-1}$ for RT38, and the lowest thermal conductivity was measured as 0.07 $W{\cdot}m^{-1}{\cdot}K^{-1}$ for SP31.

The PCM mixture experiments revealed;

- PCMs of the same family (RTHC series) can be used as mixtures.
- The melting temperature of the mixture is related to the proportion of the PCMs, which could be adjusted.
- PCMs from different families result in heterogenous mixtures and a proper phase change temperature cannot be achieved.
- When SP31 heated above its operation limit (60 °C), it loses its phase change capabilities for 24 h. Which is an important factor that shows the operating conditions should be in agreement with the characteristics of PCMs.

The experiments conducted with plastic containers uncovered;

- Incorporated copper foam reduced thermal management performance for constant discharge, however for cyclic behavior it achieved better performance compared to sole PCMs due to its high conductivity.
- For 1C rate and cyclic discharge similar behavior observed for both PCM alternatives, where 10 °C decrease in the end time temperature is achieved and latent heat capacity were not completely used. In both cases, RT25HC was able to keep the cell cooler.
- For 2C rate case, both alternatives were able to reduce the end time temperature by 20 °C. In this high load condition, RT35HC decreases the maximum temperature.
- Temperature distribution across the battery is more uniform with RT35HC in all three cases, which is essential for battery health.
- In cooling period the battery reaches the room temperature in 9 h regardless of whether a PCM is used or not. However, high thermal gradients observed in the lack of PCM introduce thermal stress on the battery. There is no sensible effect in the cooling performance for PCM blocks with or without copper foam.

Finally, passive cooling with PCM is compared with mixed cooling (PCM + Liquid cooling), the experiments show the mixed cooling is more effective than passive cooling; however, complexity increment should be considered. The experiments reveal that the liquid cooling dominates as no sensible variation could be observed with distinct PCMs.

CRediT authorship contribution statement

Umut Ege Samancıoğlu: Writing – original draft, Methodology, Investigation, Formal analysis. **Sinan Göçmen:** Writing – original draft, Methodology, Investigation, Conceptualization. **Seyed Saeed Madani:** Writing – original draft, Methodology, Investigation, Conceptualization. **Carlos Ziebert:** Writing – review & editing, Writing – original draft, Supervision, Funding acquisition, Conceptualization. **Fernando Nuno:** Writing – review & editing, Supervision, Funding acquisition, Conceptualization. **Jack Huang:** Writing – original draft, Methodology, Investigation, Conceptualization. **Frank Gao:** Writing – original draft, Methodology, Investigation, Conceptualization. **Erdal Çetkin:** Writing – review & editing, Supervision, Project administration, Methodology, Funding acquisition, Conceptualization.

Declaration of competing interest

The authors declare that they have no known competing financial interests or personal relationships that could have appeared to influence the work reported in this paper.

Acknowledgments

This work is fulfilled within the framework of the HELIOS Project (https://www.helios-h2020project.eu/project) which received funding from the European Union's Horizon 2020 research and innovation programme under grant agreement No 963646. In addition this research was partly funded by the Helmholtz Association, grant number FE.5341.0118.0012, in the program Materials and Technologies for the Energy Transition (MTET). We want to express our gratitude for the funding. This work contributes to the research performed at CELEST (Center of Electrochemical Energy Storage Ulm-Karlsruhe).

Data availability

Data will be made available on request.

References

[1] H. Jouhara, A.G. Olabi, Editorial: industrial waste heat recovery, Energy 160 (2018) 1–2, https://doi.org/10.1016/j.energy.2018.07.013.
[2] A. Foley, A.G. Olabi, Renewable energy technology developments, trends and policy implications that can underpin the drive for global climate change, Renew. Sust. Energ. Rev. 68 (2017) 1112–1114, https://doi.org/10.1016/j.rser.2016.12.065.
[3] J. Jaguemont, L. Boulon, Y. Dubé, A comprehensive review of Lithium-ion batteries used in hybrid and electric vehicles at cold temperatures, Appl. Energy 164 (2016) 99–114, https://doi.org/10.1016/j.apenergy.2015.11.034.
[4] International Energy Agency, Global EV Outlook 2021. https://www.iea.org/reports/global-ev-outlook-2021. (Accessed 29 September 2023).
[5] J. Yang, C. Hu, H. Wang, K. Yang, J.B. Liu, H. Yan, Review on the research of failure modes and mechanism for lead-acid batteries, Int. J. Energy Res. 41 (3) (2017) 336–352, https://doi.org/10.1002/er.3613.
[6] W.A. Lynch, Z.M. Salameh, Taper charge method for a nickel-cadmium electric vehicle traction battery, in: 2007 IEEE Power Engineering Society General Meeting, IEEE, 2007, pp. 1–5, https://doi.org/10.1109/PES.2007.386271.
[7] W. Wu, S. Wang, W. Wu, K. Chen, S. Hong, Y. Lai, A critical review of battery thermal performance and liquid based battery thermal management, Energy Convers. Manag. 182 (2019) 262–281, https://doi.org/10.1016/j.enconman.2018.12.051.
[8] S. Gungor, S. Gocmen, E. Cetkin, A review on battery thermal management strategies in Lithium-ion and post-lithium batteries for electric vehicles, J. Therm. Eng. (2023) 1078–1099, https://doi.org/10.18186/thermal.1334238. Yildiz Technical University.
[9] M. Ghalkhani, F. Bahiraei, G.-A. Nazri, M. Saif, Electrochemical–thermal model of pouch-type lithium-ion batteries, Electrochim. Acta 247 (2017) 569–587, https://doi.org/10.1016/j.electacta.2017.06.164.
[10] H. Feng, D. Song, A health indicator extraction based on surface temperature for lithium-ion batteries remaining useful life prediction, J. Energy Storage 34 (2021) 102118, https://doi.org/10.1016/j.est.2020.102118.
[11] E. Hosseinzadeh, R. Genieser, D. Worwood, A. Barai, J. Marco, P. Jennings, A systematic approach for electrochemical-thermal modelling of a large format lithium-ion battery for electric vehicle application, J. Power Sources 382 (2018) 77–94, https://doi.org/10.1016/j.jpowsour.2018.02.027.
[12] M. Keyser, A. Pesaran, Q. Li, S. Santhanagopalan, K. Smith, E. Wood, S. Ahmed, I. Bloom, E. Dufek, M. Shirk, A. Meintz, C. Kreuzer, C. Michelbacher, A. Burnham, T. Stephens, J. Francfort, B. Carlson, J. Zhang, R. Vijayagopal, K. Hardy, F. Dias, M. Mohanpurkar, D. Scoffield, A.N. Jansen, T. Tanim, A. Markel, Enabling fast charging – battery thermal considerations, J. Power Sources 367 (2017) 228–236, https://doi.org/10.1016/j.jpowsour.2017.07.009.
[13] A. Väyrynen, J. Salminen, Lithium ion battery production, J. Chem. Thermodyn. 46 (2012) 80–85, https://doi.org/10.1016/j.jct.2011.09.005.
[14] T.M. Bandhauer, S. Garimella, T.F. Fuller, A critical review of thermal issues in lithium-ion batteries, J. Electrochem. Soc. 158 (3) (2011) R1, https://doi.org/10.1149/1.3515880.

[15] A.A. Pesaran, Battery thermal models for hybrid vehicle simulations, J. Power Sources 110 (2) (2002) 377–382, https://doi.org/10.1016/S0378-7753(02)00200-8.
[16] A. Pesaran, Battery thermal management in EVs and HEVs: issues and solutions, Battery Man (2001) 43.
[17] M.S. Isfahani, A. Gharehghani, S. Saeedipour, M. Rabiei, PCM/metal foam and microchannels hybrid thermal management system for cooling of Li-ion battery, J. Energy Storage 72 (2023) 108789, https://doi.org/10.1016/j.est.2023.108789.
[18] C. Alaoui, Passive/active BTMS for EV lithium-ion batteries, IEEE Trans. Veh. Technol. 67 (5) (2018) 3709–3719, https://doi.org/10.1109/TVT.2018.2791359.
[19] M.M. Khan, M. Alkhedher, M. Ramadan, M. Ghazal, Hybrid PCM-based thermal management for lithium-ion Batteries: trends and challenges, J. Energy Storage 73 (2023) 108775, https://doi.org/10.1016/j.est.2023.108775.
[20] İ.G. Demirkıran, L.A.O. Rocha, E. Cetkin, Emergence of asymmetric straight and branched fins in horizontally oriented latent heat thermal energy storage units, Int. J. Heat Mass Transf. 189 (2022) 122726, https://doi.org/10.1016/j.ijheatmasstransfer.2022.122726.
[21] S. Mousavi, M. Siavashi, A. Zadehkabir, A new design for hybrid cooling of Li-ion battery pack utilizing PCM and mini channel cold plates, Appl. Therm. Eng. 197 (2021) 117398, https://doi.org/10.1016/j.applthermaleng.2021.117398.
[22] W. Wu, J. Liu, M. Liu, Z. Rao, H. Deng, Q. Wang, X. Qi, S. Wang, An innovative battery thermal management with thermally induced flexible phase change material, Energy Convers. Manag. 221 (2020) 113145, https://doi.org/10.1016/j.enconman.2020.113145.
[23] Y. Li, Y. Du, T. Xu, H. Wu, X. Zhou, Z. Ling, Z. Zhang, Optimization of thermal management system for Li-ion batteries using phase change material, Appl. Therm. Eng. 131 (2018) 766–778, https://doi.org/10.1016/j.applthermaleng.2017.12.055.
[24] U. Iqbal, M. Ali, H.A. Khalid, A. Waqas, M. Mahmood, N. Ahmed, N. Shahzad, N. Iqbal, K. Mehboob, Experimental study to optimize the thermal performance of Li-ion cell using active and passive cooling techniques, J. Energy Storage 70 (2023) 108013, https://doi.org/10.1016/j.est.2023.108013.
[25] N. Javani, I. Dincer, G.F. Naterer, B.S. Yilbas, Heat transfer and thermal management with PCMs in a Li-ion battery cell for electric vehicles, Int. J. Heat Mass Transf. 72 (2014) 690–703, https://doi.org/10.1016/j.ijheatmasstransfer.2013.12.076.